Embedding formulae for scattering by three-dimensional structures

E. A. Skelton[1], R. V. Craster[2], A. V. Shanin[3] & V. Valyaev[3]

[1] *Department of Mathematics, Imperial College of Science, Technology and Medicine, London SW7 2BZ, U.K.*
[2] *Department of Mathematical and Statistical Sciences, University of Alberta, Edmonton, Alberta, T6G 2G1, Canada*
[3] *Department of Physics (Acoustics Division), Moscow State University, 119992, Leninskie Gory, Moscow, Russia*

Abstract

The far field diffraction behaviour for canonical scattering problems involving corners or sectors, in three-dimensions, are considered. The far-field results are obtained using ideas based upon embedding formulae and therefore complement and extend existing results. Specific geometries such as the flat cone and a corner formed by a solid octant are considered in detail. The formulae derived for the diffraction behaviour are also computed in special cases and compared with known results.

Key words: Diffraction by cones; Embedding formulae

1 Introduction

The diffraction of waves by a sharp edge is a fundamental problem in many areas: fracture mechanics, radar cross-section measurements, non-destructive evaluation of structures and acoustic wave scattering, and much work has taken place on characterising the far field scattered by canonical objects: a half-plane, a wedge or a cone for use in conjunction with Keller's geometrical ray theory of diffraction [1]. Two-dimensional structures such as wedges or half-planes are typically approached using the Sommerfeld integral [2] or the Weiner-Hopf technique [3] and there is a vast literature extracting the far-fields for various canonical scattering geometries. However, in three-dimensions much less has been done, although naturally cones of circular cross-section [4,5] do allow for some simplification and can be approached through Kantorovich-Lebedev transforms; other shapes such as elliptical cross-section cones can also be tackled [6,7] and this includes the degenerate case of a flat-cone. General

three-dimensional corners and the flat-cone (a sector of a plane) can be tack-led using an approach pioneered by Smyshlyaev and co-workers [8–10]. Their approach is to extract the far-field using properties of the Laplace-Beltrami operator on the unit sphere and the far field is represented as a contour integral involving the spherical Green's function of the Laplace-Beltrami operator. Numerical evaluation of the far-field is not easy, [10,11], and can be time-consuming. As noted by one of us, [12], for a flat quarter plane computations are optimised using embedding formulae. In this case one has to evaluate the far-field created by an edge Green's function and from it construct the far field for any plane wave incidence, thus after solving a single "master" canonical problem the others are then just a manipulation of this. In the current article we build upon [12] showing that similar ideas can be used for a planar sector of any angle, and we also extend the ideas to fully three-dimensional shapes such as the edge of a cube (a solid octant). The latter extension relies upon the higher order operators introduced in [13] for wedge geometries and illustrate how the two-dimensional ideas used there translate into three dimensions.

Embedding formulae are a relatively new addition to the techniques utilised in diffraction theory: the fundamental idea is that instead of solving, and re-solving, the physical problem of interest for each different incoming plane wave angle of incidence, instead one solves a single (or much reduced number of) canonical problem(s). Then one constructs the far field of the physical problem just in terms of the canonical far field. Thus, numerically one need only solve the canonical problems, the subsequent manipulations are then a trivial numerical exercise. The method emerged for scattering by planar strips (cracks) in two-dimensional acoustics and initially utilised integral equation techniques. Williams [14] showed that, for a finite straight rigid strip, the directivity for all incident angles is obtained from just that found for a plane wave incident at the grazing angle. It is a rather remarkable result that hints at some deeper result buried within the governing equation and associated boundary conditions. Building on this framework several authors pursued this integral equation approach for a variety of scattering problems [15–21]. The approach taken in the current article follows a slightly different route. In [22] it was shown that embedding formulae emerge directly from the governing equations independent of the solution procedure and three dimensional objects could also be embedded (see also [12]). The approach utilises reciprocity, the introduction of a differential operator that generates an eigensolution that has edge conditions that are more singular than usual, and uniqueness. The canonical problem requires an edge Green's function with, in two (three) dimensions, a line (point) source placed on the sharp edges. For straight and parallel cracks or strips the number of canonical solutions is equal, in the absence of any symmetries, to the number of edges in two-dimensions. More recently [13,23] extended embedding formulae to wedge and angular geometries (of rational angle) or to cracks inclined at angles to each other, although this is still in two-dimensions. The overly singular edge Green's function ap-

2

proach is arguably a bit awkward to use with existing numerical schemes and [24] demonstrates how linear superposition can be used to create embedding formulae using the far fields from problems involving incoming plane waves. The current article takes the ideas utilised in [13], namely the higher order operators required for wedge geometries, and shows how they can be used to generate embedding formulae for some three dimensional structures namely planar sectors and an octant; the planar sectors are a generalisation of the quarter plane result [12] to any angle. To illustrate the utility of the formulae derived we evaluate the far-field numerically for the sector and compare it with that derived in [8–10].

The structure of this article is as follows: To illustrate the ideas behind embedding formulae and the three-dimensional extension we begin in section 2 with the flat cone. This is an extension of the quarter-plane treated in [12] to a sector of any angle ($< \pi$). Crucial to the embedding methodology are edge Green's functions, described in section 2.1.1 and a differential operator that transforms the standard problem into an overly singular eigensolution. The differential operator takes different forms and can be of either first or second order. Sections 2.1.2-2.1.4 illustrate this and generate the appropriate embedding formulae. A brief numerical verification and comparison of the embedding formulae versus the standard diffraction results is undertaken in section 2.2. The flat cone is quasi-two-dimensional, and closely related to the quarter-plane, and so we move on to consider fully three-dimensional corner structures. In section 3 a corner formed by a solid octant is considered and operators utilised in [13] for right-angled wedges (in two-dimensions) are used. Edge Green functions (section 3.1.1) again play a vital role and embedding formulae are again deduced. We briefly discuss extensions to yet more general geometries showing that the embedding idea is not restricted to simple geometries; this and some closing remarks are in section 4.

2   The Flat Cone

For time-harmonic motion, where the variables are proportional to $\mathrm{e}^{-\mathrm{i}\Omega t}$, the wave equation becomes the Helmholtz equation

$$(\nabla^2 + k_0^2)u = 0, \tag{2.1}$$

with $k_0 = \Omega/c$, and c the wave speed. In the first problem considered here the Helmholtz equation is satisfied everywhere in 3-dimensional space, described by Cartesian coordinates (x, y, z). A flat cone scatterer, shown in figure 1, is present in the form of a sector of a plane, $x > 0$, $0 < y < x \tan \Theta$, $z = 0$, upon which the Dirichlet condition
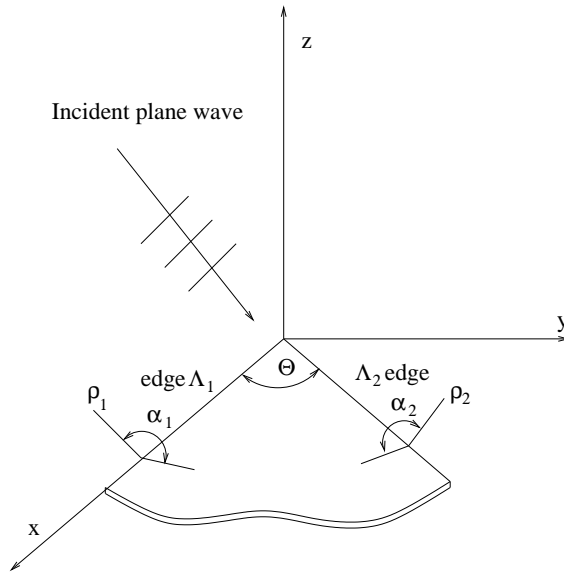
$$u = 0 \tag{2.2}$$

3

Fig. 1. The planar sector showing the notation used for angles.

is satisfied. The lines

$$x > 0, \qquad y = 0, \qquad z = 0, \text{ and} \tag{2.3}$$
$$x > 0, \quad y = x \tan \Theta, \quad z = 0, \tag{2.4}$$

are the edges of the sector, and are denoted by Λ_1 and Λ_2, respectively. The angle between the edges is Θ. Hence, when $\Theta = \pi/2$ this reduces to the problem addressed by Shanin [12].

The incident field is the plane wave

$$u^{in} = \exp[-\mathrm{i}(k_x x + k_y y + k_z z)] \tag{2.5}$$

where $k_0^2 = k_x^2 + k_y^2 + k_z^2$, and, as in [12], the edge conditions from the theory of diffraction by an ideal half-plane are

$$u \sim \rho_{1,2}^{\frac{1}{2}} \sin\left(\frac{\alpha_{1,2}}{2}\right) \tag{2.6}$$

where $\rho_{1,2}$ and $\alpha_{1,2}$ are local cylindrical radial and angular coordinates measured from the edges Λ_1 and Λ_2, respectively.

The vertex conditions, [12], are

$$u = O(1), \quad \nabla u = o(r^{-\frac{1}{2}}) \quad \text{as} \quad r \to 0, \tag{2.7}$$

and these ensure that the energy remains locally finite.

The total field u consists of the incident plane wave and a scattered field. Overall the scattered field has complicated structure, due to plane wave scat-

4

tering at the surface, and diffraction around the edges and the vertex. In the far-field the leading order terms of the scattered field are identified as a plane wave present in the geometric scattered region, together with a diffracted term decaying as $1/r$ as $r \to \infty$ where r is the distance from the vertex, together with higher order terms. Thus the diffracted term has the form

$$u(\omega, r) = 2\pi \frac{e^{ik_0 r}}{k_0 r} f(\omega) + O(e^{ik_0 r}(k_0 r)^{-2}), \qquad (2.8)$$

where ω represents the angular coordinates of the observation point (e.g. spherical polar coordinates). The diffraction coefficient $f(\omega)$ also depends on the angle of incidence of the plane wave, ω_0, and to make that explicit it is convenient to write

$$f = f(\omega; \omega_0). \qquad (2.9)$$

The objective of this paper is to find expressions for the diffraction coefficient $f(\omega; \omega_0)$ in terms of the edge Green's functions for the problem. Hence, if the far-field edge Green's functions are known everywhere, the solution to the scattering problem is constructed for any combination of angle of incidence and observation, without the need to re-solve the problem each time.

2.1 Flat Cone Embedding Formulae

We begin with the flat cone (planar sector) and demonstrate that different embedding formulae are found for various operators and provide a brief numerical comparison with results from the standard approach.

2.1.1 Edge Green's functions

Edge Green's functions, $G_x(x, y, z; X)$ and $G_s(x, y, z; S)$, are introduced via a limit process. For $G_x(x, y, z; X)$ this is achieved by placing a point source of strength $\sqrt{\pi/\epsilon}$ in the plane of the scattering cone, at a small distance ϵ away from the edge Λ_1, with X the distance from the vertex to the nearest point on the edge to the source, and taking the limit as $\epsilon \to 0$:

$$\left(\nabla^2 + k_0^2\right) \hat{G}_x(x, y, z; X, \epsilon) = \sqrt{\frac{\pi}{\epsilon}} \delta(x - X) \delta(y + \epsilon) \delta(z), \qquad (2.10)$$

$$\hat{G}_x(x, y, z; X, \epsilon) = 0 \quad \text{on} \quad x > 0,\ 0 < y < x \tan \Theta,\ z = 0, \qquad (2.11)$$

$$\hat{G}_x(x, y, z; X, \epsilon) \sim \rho_{1,2}^{\frac{1}{2}} \sin\left(\frac{\alpha_{1,2}}{2}\right) \quad \text{on} \quad \Lambda_{1,2}, \qquad (2.12)$$

$$\hat{G}_x(x, y, z; X, \epsilon) = O(1), \quad \nabla \hat{G}_x = o(r^{-\frac{1}{2}}) \quad \text{as} \quad r \to 0, \qquad (2.13)$$

5

and
$$G_x(x, y, z; X) = \lim_{\epsilon \to 0} \hat{G}_x(x, y, z; X, \epsilon). \tag{2.14}$$

In the following analysis, the local behaviour of $G_x(x, y, z; X)$ near the edge Λ_1 is required, and in particular the behaviour there of integrals of the type

$$I(x, y, z) = \int_0^\infty h(X) G_x(x, y, z; X) \mathrm{d}X. \tag{2.15}$$

This local result is given in [12], as

$$I(x, \rho_1, \alpha_1) = -\frac{h(x)}{\sqrt{\pi}} \rho_1^{-\frac{1}{2}} \sin\left(\frac{\alpha_1}{2}\right) + O\left(\rho_1^{\frac{1}{2}} \sin\left(\frac{\alpha_1}{2}\right)\right), \quad \text{near } \Lambda_1. \tag{2.16}$$

It is a special case of the result (A.9), for a point source near an infinitely long wedge, with $r_0 = \epsilon$, $\theta_0 = \pi$ and source strength $\sqrt{\pi/\epsilon}$ rather than -4π, (the leading order term), together with a term 'source-free' on the edge Λ_1 and represents the field scattered by the edge Λ_2, (the $O(\sqrt{\rho_1})$ term).

The Green's function corresponding to the other edge, Λ_2, $G_s(x, y, z; S)$, is defined in a similar way, with s being the co-ordinate measured from the origin along the edge Λ_2, and the argument S is the distance from the origin along that edge of the source.

It is convenient to define some further notation here. Following Shanin [12], the directivities f_x and f_s of the edge Green's functions are defined from their far-field asymptotic expansions as

$$G_x(x, y, z; X) = 2\pi \frac{\mathrm{e}^{\mathrm{i}k_0 r}}{k_0 r} f_x(\omega; X) + O\left(\mathrm{e}^{\mathrm{i}k_0 r}(k_0 r)^{-2}\right), \tag{2.17}$$

$$G_s(x, y, z; S) = 2\pi \frac{\mathrm{e}^{\mathrm{i}k_0 r}}{k_0 r} f_s(\omega; S) + O\left(\mathrm{e}^{\mathrm{i}k_0 r}(k_0 r)^{-2}\right), \tag{2.18}$$

and by symmetry

$$G_x(x, y, z; X) = G_s(x \cos \Theta + y \sin \Theta, x \sin \Theta - y \cos \Theta, z; X), \tag{2.19}$$
$$f_x(\xi, \eta; X) = f_s(\xi \cos \Theta + \eta \sin \Theta, \xi \sin \Theta - \eta \cos \Theta; X), \tag{2.20}$$

in which (ξ, η) are "Cartesian" co-ordinates

$$\xi = \sin \theta \cos \phi, \quad \eta = \sin \theta \sin \phi, \tag{2.21}$$

representing the projection of the point ω on the x-y plane. Additionally, the asymptotic behaviour of the edge Green's functions, G_s and G_x, near the opposite edges, Λ_1 and Λ_2, respectively, are

6

$$G_s(x, \rho_1, \alpha_1; S) = \frac{2C_G(x; S)}{\sqrt{\pi}} \rho_1^{\frac{1}{2}} \sin \frac{\alpha_1}{2} + O\left(\rho_1^{\frac{3}{2}}\right), \quad \text{near } \Lambda_1, \tag{2.22}$$

$$G_x(s, \rho_2, \alpha_2; X) = \frac{2C_G(s; X)}{\sqrt{\pi}} \rho_2^{\frac{1}{2}} \sin \frac{\alpha_2}{2} + O\left(\rho_2^{\frac{3}{2}}\right), \quad \text{near } \Lambda_2, \tag{2.23}$$

where (ρ_1, α_1, x), (ρ_2, α_2, s) are cylindrical polar co-ordinate systems with Λ_1, Λ_2 respectively being the axis. Reciprocity allows the position of source and observer to be interchanged, hence

$$C_G(x; s) = C_G(s; x). \tag{2.24}$$

2.1.2 Embedding formula using the operator $H_x = \partial/\partial x + \mathrm{i}k_x$

The embedding technique developed in [22]—[23] is applied here. Briefly, this entails finding an operator that, when applied to the total field of the original problem, produces a new field that satisfies the original equations, the boundary conditions, the radiation condition and which has the appropriate asymptotic behaviour near to any edges to ensure that it is 'source-free' there. When these properties are satisfied, uniqueness arguments apply to show that the new field is identically zero everywhere. Far-field asymptotic analysis of the formal definition of the new field then allows an expression for the directivity of the original scattered field to be extracted. In this section the operator

$$H_x = \frac{\partial}{\partial x} + \mathrm{i}k_x, \tag{2.25}$$

which has been used successfully in the past, [22], is applied to the total field u. The resulting field $H_x[u]$ has the following properties:

(1) $H_x[u]$ satisfies the Helmholtz equation
(2) $H_x[u]$ satisfies the Dirichlet boundary condition on the surfaces of the scatterer
(3) $H_x[u^{in}] \equiv 0$ and hence $H_x[u] = H_x[u^s]$, in which u^s is the outgoing scattered field of the original problem. Thus $H_x[u]$ also satisfies the radiation condition.

However, the remaining requirement that the new field should have the correct 'source-free' behaviour at the edges ($\sim \rho_{1,2}^{\frac{1}{2}}$ as in equation (2.6)), although met on Λ_1, is not met on Λ_2, as shown below: From equation (2.6) the field near Λ_1 is expressed in the form

$$u(x, \rho_1, \alpha_1) = \frac{2C_x(x)}{\sqrt{\pi}} \rho_1^{\frac{1}{2}} \sin \frac{\alpha_1}{2} + o(\rho_1^{\frac{1}{2}}) \quad \text{near } \Lambda_1, \tag{2.26}$$

7

in which $C_x(x)$ is an as yet unknown function of x. Hence

$$H_x[u] = \frac{2\left(C_x'(x) + ik_x C_x(x)\right)}{\sqrt{\pi}} \rho_1^{\frac{1}{2}} \sin\frac{\alpha_1}{2} + o(\rho_1^{\frac{1}{2}}) \quad \text{near } \Lambda_1, \tag{2.27}$$

which has the required $\rho_1^{\frac{1}{2}}$ behaviour. Similarly, near to Λ_2 the field is

$$u(s, \rho_2, \alpha_2) = \frac{2C_s(s)}{\sqrt{\pi}} \rho_2^{\frac{1}{2}} \sin\frac{\alpha_2}{2} + o(\rho_2^{\frac{1}{2}}). \tag{2.28}$$

Differentiation with respect to x is accomplished by considering a rotation of the x and y axes through angle Θ, so they correspond with the s axis and perpendicular to it a $\tilde{t}$ axis, such that

$$\rho_2^2 = \tilde{t}^2 + z^2, \quad \tan\alpha_2 = -z/\tilde{t}, \tag{2.29}$$

and

$$s = x\cos\Theta + y\sin\Theta, \quad \tilde{t} = -x\sin\Theta + y\cos\Theta. \tag{2.30}$$

Performing the differentiation gives, near Λ_2

$$H_x[u] = \frac{-\sin\Theta C_s(s)}{\sqrt{\pi}} \rho_2^{-\frac{1}{2}} \sin\frac{\alpha_2}{2} + O\left(\rho_2^{\frac{1}{2}}\right) \tag{2.31}$$

and hence $H_x[u]$ does not have the required behaviour there and so, in this particular example, appears to fail the required criteria for generating embedding formulae. However, from equations (2.15) and (2.16) another expression can be constructed with this leading order behaviour near to Λ_2:

$$\sin\Theta \int_0^\infty C_s(S)G_s(x, y, z; S)\mathrm{d}S = \frac{-\sin\Theta C_s(s)}{\sqrt{\pi}} \rho_2^{-\frac{1}{2}} \sin\frac{\alpha_2}{2} + O\left(\rho_2^{\frac{1}{2}}\right), \tag{2.32}$$

and hence, by defining,

$$u^* = H_x[u] - \sin\Theta \int_0^\infty C_s(S)G_s(x, y, z; S)\mathrm{d}S, \tag{2.33}$$

a function is constructed which has the required asymptotic behaviour near the edge Λ_2. The second term above is a superposition of Green's functions with sources along the edge Λ_2, each of which satisfies the Helmholtz equation, the boundary conditions on the scatterer faces, and has the required edge behaviour near to Λ_1. Importantly, after a detailed study one can prove that the vertex condition is also satisfied. Hence the combination of terms u^* satisfies all the requirements needed for the embedding method. Then, from uniqueness arguments

$$u^* \equiv 0 \tag{2.34}$$

and

$$H_x[u(x, y, z)] = \sin\Theta \int_0^\infty C_s(S)G_s(x, y, z; S)\mathrm{d}S. \tag{2.35}$$

8

This is the weak form of the embedding formula, and corresponds to Shanin's [12] equation (18) for a cone with angle $\pi/2$, but now generalised to a cone of general angle Θ.

The, at present, unknown function C_s is determined using a reciprocity argument, between a point source of strength $\sqrt{\pi/\epsilon}$ used in the definition of $\hat{G}_s$ (and hence in the limiting case as $\epsilon \to 0$ of G_s) at distance S along edge Λ_2 and a point at angular location ω_0 at distance r in the far-field. The leading order term of the far-field due to the source with this amplitude located near to Λ_2, G_{21} say, is obtained directly from equation (2.18)

$$G_{21} \sim 2\pi \frac{e^{ik_0 r}}{k_0 r} f_s(\omega_0; S). \tag{2.36}$$

If the source is located in the far-field then, near the vertex of the scatterer the incident field from the source is approximately that of a plane wave of amplitude $-\sqrt{\pi/\epsilon} e^{ik_0 r}/4\pi r$. Hence the leading order term of the total field near the point S on Λ_2, u_{12} say, is obtained, by comparison with equation (2.28) which is for a plane wave of unit amplitude, as

$$u_{12} \sim -\sqrt{\frac{\pi}{\epsilon}} \frac{e^{ik_0 r}}{4\pi r} \frac{2C_s(s)}{\sqrt{\pi}} \rho_2^{\frac{1}{2}} \sin \frac{\alpha_2}{2} \quad \text{near } \Lambda_2. \tag{2.37}$$

At the point under discussion, $s = S$, $\rho_2 = \epsilon$ and $\alpha_2 = \pi$, hence

$$G_{12} \sim -\sqrt{\frac{\pi}{\epsilon}} \frac{e^{ik_0 r}}{4\pi r} \frac{2C_s(S)}{\sqrt{\pi}} \sqrt{\epsilon} = \frac{-e^{ik_0 r} C_s(S)}{2\pi r}. \tag{2.38}$$

Applying the reciprocity principle, that the same result is obtained if the source and observer positions are interchanged, shows that

$$G_{12} = G_{21} \tag{2.39}$$

and hence an expression for the unknown function $C_s(S)$ is obtained as

$$C_s(S) = -\frac{(2\pi)^2}{k_0} f_s(\omega_0; S), \tag{2.40}$$

allowing equation (2.35) to be expressed as

$$H_x[u(x, y, z)] = \frac{-(2\pi)^2 \sin \Theta}{k_0} \int_0^\infty f_s(\omega_0; S) G_s(x, y, z; S) dS. \tag{2.41}$$

After noting that in the far-field $\partial/\partial x$ corresponds to $ik_0\xi$, the far-field approximation of this equation results in the embedding formula

$$f(\omega; \omega_0) = \frac{4\pi^2 i \sin \Theta}{k_0^2(\xi + \xi_0)} \int_0^\infty f_s(\omega_0; S) f_s(\omega; S) dS. \tag{2.42}$$

9

corresponding to Shanin's [12] equation (12) in the limit as the sector angle is $\pi/2$, but now generalised to a flat cone of general angle Θ.

2.1.3 Using the operator $H_y = \partial/\partial y + \mathrm{i}k_y$

In [12] Shanin also presents a first order embedding formula based on the operator H_y for the problem of scattering by a quarter plane. This is particularly appropriate to that geometry since the y-axis is the second edge of the scatterer and the result follows immediately by symmetry. This is not the case for a scatterer of arbitrary angle, considered here.

It is clear that the field defined by $H_y[u]$ satisfies the requirements listed as 1–3 of the previous subsection, but in this case it fails the requirement of the edge behaviour, not only on Λ_2 but also on Λ_1. Fortunately a slight modification allows us to subtract the singular behaviour along both of the edges, setting

$$u^* = H_y[u] - \int_0^\infty C_x(X)G_x(x,y,z;X)\mathrm{d}X + \cos\Theta \int_0^\infty C_s(S)G_s(x,y,z;S)\mathrm{d}S,$$
$$(2.43)$$

produces a field satisfying all the requirements for the embedding method. Thus

$$u^* \equiv 0, \qquad (2.44)$$

and

$$H_y[u(x,y,z)] = \int_0^\infty C_x(X)G_x(x,y,z;X)\mathrm{d}X - \cos\Theta \int_0^\infty C_s(S)G_s(x,y,z;S)\mathrm{d}S,$$
$$(2.45)$$

as the weak form of the embedding formula for this operator. Equation (2.40) relating $C_s(S)$ and $f_s(\omega_0;S)$, derived previously, holds in this case too, together with the corresponding equation relating $C_x(X)$ and $f_x(\omega_0;X)$. Substituting these into equation (2.45) and applying the far-field approximation results in the embedding formula

$$f(\omega;\omega_0) = \frac{4\pi^2\mathrm{i}}{k_0^2(\eta+\eta_0)}\left\{\int_0^\infty f_x(\omega_0;X)f_x(\omega;X)\mathrm{d}X - \cos\Theta\int_0^\infty f_s(\omega_0;S)f_s(\omega;S)\mathrm{d}S\right\},$$
$$(2.46)$$

corresponding to Shanin's [12] equation (13) for a cone with angle $\pi/2$, but now generalised to a cone of general angle Θ.

Similarly we can use the operator $H_s = \partial/\partial s + \mathrm{i}k_0(\xi_0\cos\Theta + \eta_0\sin\Theta)$ as a rotation of axes gives

$$H_s[u] = \cos\Theta H_x[u] + \sin\Theta H_y[u] = \sin\Theta\int_0^\infty C_x(X)G_x(x,y,z;X)\mathrm{d}X, \quad (2.47)$$

10

to get

$$f(\omega; \omega_0) = \frac{4\pi^2 i \sin \Theta}{k_0^2 \left(\cos \Theta (\xi + \xi_0) + \sin \Theta (\eta + \eta_0) \right)} \int_0^\infty f_x(\omega_0; X) f_x(\omega; X) \mathrm{d}X,$$

(2.48)

which could also be considered to correspond to Shanin's [12] equation (13) for a cone with angle $\pi/2$, but generalised to a cone of general angle Θ.

2.1.4 Using a "second order" operator

Embedding formulae are also obtained using suitable higher order operators, provided the requirements outlined above are met. In [12] the second order operator $H_{xy}[u] = H_x[H_y[u]]$ is used to obtain a different embedding formula for the right angled flat cone. Here, for a flat cone with angle Θ a corresponding embedding formula is obtained using the operator

$$H_{xs} = \left(\frac{\partial}{\partial x} + i k_0 \xi_0 \right) \left(\frac{\partial}{\partial s} + i k_0 (\xi_0 \cos \Theta + \eta_0 \sin \Theta) \right).$$

(2.49)

The asymptotic behaviour near the Λ_2 edge is found, from equations (2.31) and (2.32), to be

$$H_{xs}[u] \sim - \left(\frac{\partial}{\partial s} + i k_0 (\xi_0 \cos \Theta + \eta_0 \sin \Theta) \right) \frac{\sin \Theta C_s(s)}{\sqrt{\pi}} \rho_2^{-\frac{1}{2}} \sin \frac{\alpha_2}{2}$$

$$\sim \sin \Theta \int_0^\infty \left[\frac{\partial}{\partial S} C_s(S) + i k_0 (\xi_0 \cos \Theta + \eta_0 \sin \Theta) C_s(S) \right] G_s(x, y, z; S) \mathrm{d}S.$$

(2.50)

Similarly, near Λ_1 the asymptotic behaviour is

$$H_{xs}[u] \sim - \left(\frac{\partial}{\partial x} + i k_0 \xi_0 \right) \frac{\sin \Theta C_x(x)}{\sqrt{\pi}} \rho_1^{-\frac{1}{2}} \sin \frac{\alpha_1}{2}$$

$$\sim \sin \Theta \int_0^\infty \left[\frac{\partial}{\partial X} C_x(X) + i k_0 \xi_0 C_x(X) \right] G_x(x, y, z; X) \mathrm{d}X.$$

(2.51)

Thus a field u^* satisfying all the properties required is constructed:

$$u^* = H_{xs}[u] - \sin \Theta \int_0^\infty \left[\frac{\partial}{\partial S} C_s(S) + i k_0 (\xi_0 \cos \Theta + \eta_0 \sin \Theta) C_s(S) \right] G_s(x, y, z; S) \mathrm{d}S$$

$$- \sin \Theta \int_0^\infty \left[\frac{\partial}{\partial X} C_x(X) + i k_0 \xi_0 C_x(X) \right] G_x(x, y, z; X) \mathrm{d}X.$$

(2.52)

11

Hence, again $u^* \equiv 0$, and thus the weak form of embedding from this operator is

$$H_{xs}[u(x, y, z)] = \sin \Theta \int_0^\infty \left[\frac{\partial}{\partial S} C_s(S) + \mathrm{i}k_0 \left(\xi_0 \cos \Theta + \eta_0 \sin \Theta \right) C_s(S) \right] G_s(x, y, z; S) \mathrm{d}S$$

$$+ \sin \Theta \int_0^\infty \left[\frac{\partial}{\partial X} C_x(X) + \mathrm{i}k_0 \xi_0 C_x(X) \right] G_x(x, y, z; X) \mathrm{d}X. \qquad (2.53)$$

After noting that equation (2.40) for C_s, and the corresponding relation for C_x remain valid, and applying the far-field asymptotic expansions the embedding formula obtained using this second order operator is

$$f(\omega; \omega_0) = \frac{4\pi^2 \sin \Theta}{k_0^3 (\xi + \xi_0) \left(\cos \Theta(\xi + \xi_0) + \sin \Theta(\eta + \eta_0) \right)} \times$$

$$\left\{ \int_0^\infty \left[\frac{\partial}{\partial S} f_s(\omega_0; S) + \mathrm{i}k_0 \left(\xi_0 \cos \Theta + \eta_0 \sin \Theta \right) f_s(\omega_0; S) \right] f_s(\omega; S) \mathrm{d}S \right.$$

$$\left. + \int_0^\infty \left[\frac{\partial}{\partial X} f_x(\omega_0; X) + \mathrm{i}k_0 \xi_0 f_x(\omega_0; X) \right] f_x(\omega; X) \mathrm{d}X \right\}. \qquad (2.54)$$

This formula requires derivatives with respect to the source position of the directivities of the edge Green's functions, whose calculation requires more computational effort than the Green's functions themselves. It is therefore desirable to rearrange the formula to avoid the necessity of calculating them. This is achieved by first considering $\partial G_x(x, y, z; X)/\partial X$, which satisfies the Helmholtz equation everywhere *except* at the source position. However, the combination $\partial G_x/\partial X + \partial G_x/\partial x$ has no singularity as $x \to X$ and therefore satisfies the Helmholtz equation everywhere. Additionally it satisfies the boundary conditions on the faces of the flat cone, the radiation condition, and the edge condition on Λ_1. It does however still have singular behaviour near Λ_2, since, following the method outlined in (2.28)–(2.32), but with u replaced now with G_x and $C_s(s)$ replaced now with $C_G(s; X)$,

$$\frac{\partial G_x}{\partial x} \sim \frac{-\sin \Theta C_G(s; X)}{\sqrt{\pi}} \rho_2^{-\frac{1}{2}} \sin \frac{\alpha_2}{2} + O\left(\rho_2^{\frac{1}{2}} \right) \quad \text{near } \Lambda_2$$

$$\sim \sin \Theta \int_0^\infty C_G(S; X) G_s(x, y, z; S) \mathrm{d}S + O\left(\rho_2^{\frac{1}{2}} \right) \quad \text{near } \Lambda_2. \qquad (2.55)$$

Hence,

$$\frac{\partial G_x}{\partial X} + \frac{\partial G_x}{\partial x} - \sin \Theta \int_0^\infty C_G(S; X) G_s(x, y, z; S) \mathrm{d}S \sim O\left(\rho_2^{\frac{1}{2}} \right) \quad \text{near } \Lambda_2,$$
$$(2.56)$$

12

and the left hand side of this equation now satisfies the Helmholtz equation, the boundary conditions on the faces, the edge conditions on both edges and the radiation condition. Therefore, by a further application of the uniqueness argument it is identically zero everywhere. Thus

$$\frac{\partial G_x}{\partial X} = -\frac{\partial G_x}{\partial x} + \sin\Theta \int_0^\infty C_G(S; X) G_s(x, y, z; S) \mathrm{d}S, \qquad (2.57)$$

and in the far-field

$$\frac{\partial}{\partial X} f_x(\omega_0; X) = -\mathrm{i}k_0\xi_0 f_x(\omega_0; X) + \sin\Theta \int_0^\infty C_G(S; X) f_s(\omega_0; S) \mathrm{d}S. \quad (2.58)$$

Similarly, by considering the behaviour of $\partial G_s/\partial S + \partial G_s/\partial s$

$$\frac{\partial G_s}{\partial S} = -\frac{\partial G_s}{\partial s} + \sin\Theta \int_0^\infty C_G(X; S) G_x(x, y, z; X) \mathrm{d}X, \qquad (2.59)$$

which has the far-field form

$$\frac{\partial}{\partial S} f_s(\omega_0; S) = -\mathrm{i}k_0 \left(\xi_0 \cos\Theta + \eta_0 \sin\Theta\right) f_s(\omega_0; S) + \sin\Theta \int_0^\infty C_G(X; S) f_x(\omega_0; X) \mathrm{d}X.$$
$$(2.60)$$

Thus, by substituting (2.58) and (2.60) into the embedding formula (2.54) the embedding formula is obtained in the form of a double integral, corresponding to Shanin's [12] equation (14) as

$$f(\omega; \omega_0) = \frac{4\pi^2 \sin\Theta}{k_0^3(\xi + \xi_0)\left(\cos\Theta(\xi + \xi_0) + \sin\Theta(\eta + \eta_0)\right)} \times$$
$$\int_0^\infty \int_0^\infty \left[f_x(\omega; X) f_s(\omega_0; S) + f_x(\omega_0; X) f_s(\omega; S)\right] C_G(X; S) \mathrm{d}X \mathrm{d}S.$$
$$(2.61)$$

2.2   Numerical Results

For the embedding formulae to be of value it is important to demonstrate that they reproduce the results found using the standard formula for the directivity:

$$f(\omega; \omega_0) = \frac{i}{\pi} \int_\gamma e^{-i\pi\nu} g_r(\omega, \omega_0, \nu) \nu d\nu \qquad (2.62)$$

where g_r is the "reflected" part of the Green's function on the sphere with a cut. The details of this formula are to be found in [10]. We choose to compare this with the embedding formula (2.42) and require the edge Green's functions. The embedding formula is written in terms of the spherical edge

Green's function $v^1(\omega, \nu)$ derived in [25] as

$$f(\omega; \omega_0) =$$

$$\frac{1}{4\pi i(\eta(\omega) + \eta(\omega_0))} \int_{-i\infty-1/2}^{i\infty-1/2} (v^1(\omega, \nu)v^1(\omega_0, \nu+1) + v^1(\omega, \nu+1)v^1(\omega_0, \nu))d\nu$$

$$(2.63)$$

where $\eta(\omega) = \sin\theta(\omega)\sin(\phi(\omega))$. To allow a brief and simple comparison across several sector angles we just consider the incidence direction to be at the axis of symmetry of the cone, i.e. it has spherical coordinates $\theta = \pi/2, \phi = \pi + \Theta/2$. The scattering directions are taken in the sagittal plane, i.e. they have spherical coordinates $\theta = \theta^{\text{sc}}, \phi = \pi + \Theta/2$ for various θ^{sc}. In this case the diffraction coefficient is purely imaginary and it is plotted versus θ^{sc} in figure 2. Numerically we find that the real part of the diffraction coefficients calculated either way is extremely small. In figure 2 the embedding result and the standard result are compared and the results are visually indistinguishable the maximal difference is $\sim 3\cdot 10^{-4}$. It is naturally reassuring that the numerical comparison is easily performed and accurate.
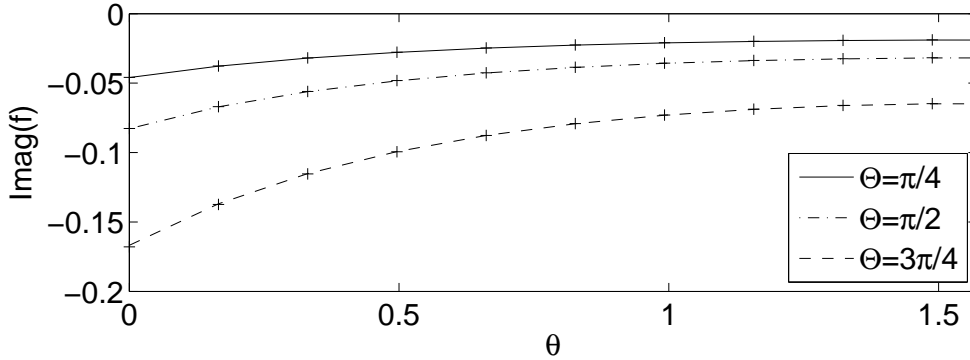

Fig. 2. Numerical results: the directivity function along the sagittal plane for three sectoral angles. The crosses are from the embedding formulae and the lines from the standard Smyshlyaev result.

3 The Solid Cone

In the second problem considered here a 3-D solid cone occupies the $1/8$ space, octant, defined by $x > 0, y > 0, z > 0$, as shown in figure 3. The cone surfaces are the three quarter planes, subtending angle $\pi/2$: (i) $x = 0, y > 0, z > 0$, S_1 say, (ii) $y = 0, x > 0, z > 0$, S_2 say, and (iii) $z = 0, x > 0, y > 0$, S_3 say, which are mutually at right angles. The edges are denoted Λ_1, the positive x-axis, $y = 0, z = 0$, Λ_2, the positive y-axis, $x = 0, z = 0$ and Λ_3, the positive z-axis, $x = 0, y = 0$. An acoustic medium occupies everywhere *except* for the octant $x > 0, y > 0, z > 0$. The incident field is a plane wave described by equation (2.5).
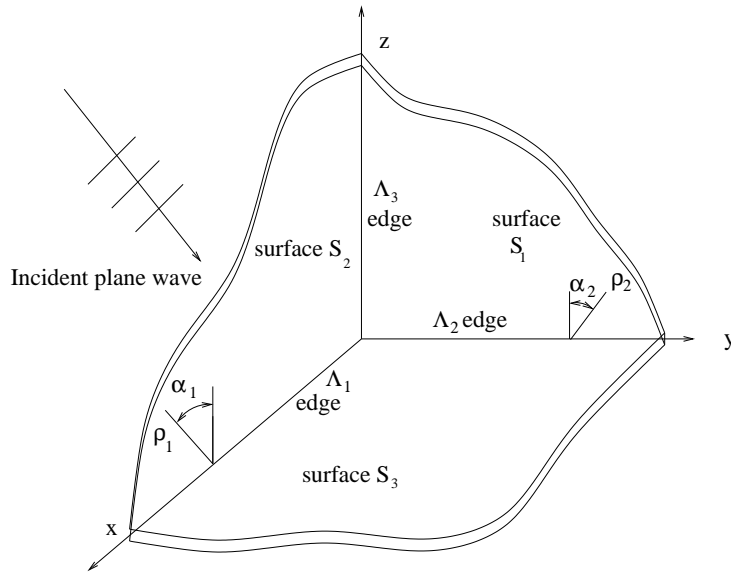
Fig. 3. Octant geometry formed by three perpendicular quarter planes.

Dirichlet boundary conditions, (2.2), are taken on the three planar surfaces of the cone and the edge conditions are obtained from the theory of diffraction by an ideal infinitely long wedge subtending an angle of $\pi/2$, as

$$u \sim \rho_{1,2,3}^{\frac{2}{3}} \sin\left(\frac{2\alpha_{1,2,3}}{3}\right) \tag{3.1}$$

where $\rho_{1,2,3}$ and $\alpha_{1,2,3}$ are local cylindrical radial and angular coordinates measured from the edges Λ_1, Λ_2 and Λ_3, respectively.

As in the previous example the total field consists of the incident field and a scattered field, which can itself be considered as a plane wave present in the geometric scattered region together with a diffracted term. The far-field of the diffracted term is again characterised by the diffraction coefficient, or directivity, $f(\omega; \omega_0)$, defined as in equation (2.8).

3.1 Solid Cone Embedding Formulae

3.1.1 Edge Green's functions

Edge Green's functions, $G_{1x}(x, y, z; X)$, $G_{1y}(x, y, z; Y)$ and $G_{1z}(x, y, z; Z)$, are now introduced via a limit process as described in detail in Appendix A. For this geometry the angle between the planes is $\pi/2$, and thus $p = 1$ and $q = 2$ in the notation used in Appendix A. For $G_{1z}(x, y, z; Z)$, for example, this is achieved by placing a point source of strength $1/\epsilon^{\frac{2}{3}}$ in the plane of the scattering cone, at a small distance ϵ away from the edge Λ_3, with Z the distance from the vertex to the nearest point on the edge to the source, and

15

taking the limit as $\epsilon \to 0$:

$$(\nabla^2 + k_0^2)\hat{G}_{1z} = 4\pi\delta(x - \epsilon/\sqrt{2})\delta(y - \epsilon/\sqrt{2})\delta(z - z_0)/\epsilon^{\frac{2}{3}} =$$

$$4\pi\delta(\rho_3 - \epsilon)\delta(\alpha_3 - \theta_0)\delta(z - z_0)/\epsilon^{\frac{2}{3}}\rho_3 \qquad (3.1)$$

where ρ_3, α_3 and z are local cylindrical polar coordinates and the fluid occupies $0 < \alpha_3 < 3\pi/2$, $\theta_0 = 3\pi/4$ and $\epsilon \to 0$. The different power of ϵ on the right hand side here compared to equation (2.10) reflects the different geometry here. These edge Green's functions must also satisfy the boundary, edge and radiation conditions required of the original problem:

$$\hat{G}_{1z}(x, y, z; Z, \epsilon) = 0 \qquad \text{on} \qquad S_{1,2,3}, \qquad (3.2)$$

$$\hat{G}_{1z}(x, y, z; Z, \epsilon) \sim \rho_{1,2,3}^{\frac{2}{3}} \sin\left(\frac{2\alpha_{1,2,3}}{3}\right) \qquad \text{on} \quad \Lambda_{1,2,3}, \qquad (3.3)$$

and

$$G_{1z}(x, y, z; Z) = \lim_{\epsilon \to 0} \hat{G}_{1z}(x, y, z; Z, \epsilon). \qquad (3.4)$$

The important local result for this Green's function, obtained from Appendix A, is that near Λ_3

$$\int_0^\infty h(Z)G_{1z}(x, y, z; Z)\mathrm{d}Z = -4h(z)\rho_3^{-\frac{2}{3}}\sin\left(\frac{2\alpha_3}{3}\right) + O\left(\rho_3^{\frac{2}{3}}\sin\left(\frac{2\alpha_3}{3}\right)\right), \qquad (3.5)$$

together with corresponding results for the integrals of $G_{1x}(x, y, z; X)$ and $G_{1y}(x, y, z; Y)$.

For this more complicated geometry we need to introduce the 'dipole edge Green's functions', $G_{2x}(x, y, z; X)$, $G_{2y}(x, y, z; Y)$ and $G_{2z}(x, y, z; Z)$, satisfying the boundary, edge and radiation conditions. and, for $G_{2z}(x, y, z; Z)$ for example,

$$(\nabla^2 + k_0^2)G_{2z} = 4\pi\delta(\rho_3 - \epsilon)\delta'(\alpha_3 - \theta_0)\delta(z - z_0)/\epsilon^{\frac{4}{3}}\rho_3 \qquad (3.6)$$

in which a shorthand notation has been used, where the limit as $\epsilon \to 0$ is now assumed. The details of the derivation and properties of these 'dipole edge Green's functions' is presented in Appendix A. The important local result for *this* dipole Green's function, corresponding to equation (3.5), is obtained from Appendix A as

$$\int_0^\infty h(Z)G_{2z}(x, y, z; Z)\mathrm{d}Z = -\frac{8}{3}h(z)\rho_3^{-\frac{4}{3}}\sin\left(\frac{4\alpha_3}{3}\right) + O\left(\rho_3^{\frac{2}{3}}\right), \quad \text{near } \Lambda_3, \qquad (3.7)$$

together with corresponding results for the integrals of $G_{2x}(x, y, z; X)$ and $G_{2y}(x, y, z; Y)$.

16

3.1.2 Using the operator $H_{2x} = \partial^2/\partial x^2 + k_x^2$

In [13] and [23] it was demonstrated that for wedge shaped geometries higher order operators were needed to construct embedding formulae than those needed for line geometries. In [13] the higher order operators H_{px} were defined as

$$H_{px} = (\mathrm{i}k_0)^p \left[T_p \left(\frac{\mathrm{i}}{k_0} \frac{\partial}{\partial x} \right) - T_p \left(\frac{k_x}{k_0} \right) \right] \tag{3.8}$$

where T_p is the Tchebychev polynomial of order p, and used for wedge geometries of more general angle. In particular for 2–D wedges with angle $\pi/2$ operators of a least second order are necessary and the operator $H_{2x} = \partial^2/\partial x^2 + k_x^2$ was used. Hence, for this problem in which the cone surfaces are all mutually perpendicular the simple second order operator H_{2x} will be used as the basis for constructing an embedding formula. The resulting field $H_{2x}[u]$ has the following properties:

(1) $H_{2x}[u]$ satisfies the Helmholtz equation.
(2) $H_{2x}[u]$ satisfies the Dirichlet boundary condition on each of the surfaces of the cone. On S_2 and S_3 $u \equiv 0$ there and hence clearly $\partial u/\partial x \equiv 0$ and $\partial^2 u/\partial x^2 \equiv 0$ there also. On S_1, since u satisfies the Helmholtz equation, $H_{2x}[u]$ is rewritten as

$$H_{2x}[u] = \left(k_x^2 - k_0^2 - \frac{\partial^2}{\partial y^2} - \frac{\partial^2}{\partial z^2} \right) u, \tag{3.9}$$

and since $u \equiv 0$ on S_1 clearly $\partial^2 u/\partial y^2 \equiv 0$ and $\partial^2 u/\partial z^2 \equiv 0$ there too.
(3) $H_{2x}[u^{in}] \equiv 0$, hence $H_{2x}[u]$ satisfies the radiation condition.

However, although this new field satisfies the edge conditions on Λ_1, it does not have 'source-free' behaviour near to the edges Λ_2 and Λ_3. For example, near to Λ_2,

$$u(y, \rho_2, \alpha_2) = C_y(y)\rho_2^{\frac{2}{3}} \sin \frac{2\alpha_2}{3} + D_y(y)\rho_2^{\frac{4}{3}} \sin \frac{4\alpha_2}{3} + o(\rho_2^{\frac{4}{3}}), \tag{3.10}$$

where the unknown functions $C_y(y)$ and $D_y(y)$ are still to be determined. Hence, after differentiating with respect to x as in §2.1, it is found that

$$H_{2x}[u] = -\frac{2}{9}C_y(y)\rho_2^{-\frac{4}{3}} \sin \frac{4\alpha_2}{3} + \frac{4}{9}D_y(y)\rho_2^{-\frac{2}{3}} \sin \frac{2\alpha_2}{3} + O(\rho_2^{\frac{2}{3}}) \quad \text{near } \Lambda_2, \tag{3.11}$$

and hence does not have the required behaviour near Λ_2. These singular combinations of ρ_2 and α_2 are precisely the terms which occur as the leading order terms of integrals similar to those of equations (3.7) and (3.5), allowing the construction of an expression which is non-singular near Λ_2:

$$H_{2x}[u] - \frac{1}{12} \int_0^\infty C_y(Y)G_{2y}(x, y, z; Y)\mathrm{d}Y + \frac{1}{9} \int_0^\infty D_y(Y)G_{1y}(x, y, z; Y)\mathrm{d}Y = O(\rho_2^{\frac{2}{3}}). \tag{3.12}$$

17

Similarly, near Λ_3

$$H_{2x}[u] = -\frac{2}{9}C_z(z)\rho_3^{-\frac{4}{3}}\sin\frac{4\alpha_3}{3} + \frac{4}{9}D_z(z)\rho_3^{-\frac{2}{3}}\sin\frac{2\alpha_3}{3} + O(\rho_3^{\frac{2}{3}}), \qquad (3.13)$$

and

$$H_{2x}[u] - \frac{1}{12}\int_0^\infty C_z(Z)G_{2z}(x,y,z;Z)\mathrm{d}Z + \frac{1}{9}\int_0^\infty D_z(Z)G_{1z}(x,y,z;Z)\mathrm{d}Z = O(\rho_3^{\frac{2}{3}}).$$
$$(3.14)$$

Hence, by combining results (3.12) and (3.14) a function u^* can be constructed for this problem as

$$u^* = H_{2x}[u] - \frac{1}{12}\int_0^\infty C_y(Y)G_{2y}(x,y,z;Y)\mathrm{d}Y + \frac{1}{9}\int_0^\infty D_y(Y)G_{1y}(x,y,z;Y)\mathrm{d}Y$$
$$-\frac{1}{12}\int_0^\infty C_z(Z)G_{2z}(x,y,z;Z)\mathrm{d}Z + \frac{1}{9}\int_0^\infty D_z(Z)G_{1z}(x,y,z;Z)\mathrm{d}Z, \qquad (3.15)$$

a combination which has the required asymptotic behaviour near all three edges Λ_1, Λ_2 and Λ_3. The additional terms added to $H_{2x}[u]$ above are all combinations of Green's functions which, away from the edges, satisfy the Helmholtz equation, the Dirichlet boundary conditions on the cone surfaces and the radiation condition. Then, applying the uniqueness argument again the function u^* is found to be identically zero everywhere and

$$H_{2x}[u(x,y,z)] = -\frac{1}{9}\int_0^\infty D_y(Y)G_{1y}(x,y,z;Y)\mathrm{d}Y + \frac{1}{12}\int_0^\infty C_y(Y)G_{2y}(x,y,z;Y)\mathrm{d}Y$$
$$-\frac{1}{9}\int_0^\infty D_z(Z)G_{1z}(x,y,z;Z)\mathrm{d}Z + \frac{1}{12}\int_0^\infty C_z(Z)G_{2z}(x,y,z;Z)\mathrm{d}Z, \qquad (3.16)$$

which is the weak form of the embedding formula for this problem.

The unknown functions $C_y(Y)$, $C_z(Z)$, $D_y(Y)$ and $D_z(Z)$ are determined using similar reciprocity arguments to those used in the previous section. Thus, for example consider a monopole point source of strength $4\pi/\epsilon^{\frac{2}{3}}$, used in the definition of $\hat{G}_{1y}$ (and hence in the limiting case as $\epsilon \to 0$ of G_{1y}) at distance Y along edge Λ_2 and the same source at angular location ω_0 at distance r in the far-field. The leading order term of the far-field due to the source near Λ_2, G_{YF} say, is obtained from its directivity

$$G_{YF} \sim 2\pi\frac{\mathrm{e}^{\mathrm{i}k_0 r}}{k_0 r}f_{1y}(\omega_0;Y). \qquad (3.17)$$

Correspondingly, if this source is located in the far-field then, near the vertex of the cone the incident field from the source is approximately that of a plane

wave of amplitude $-\mathrm{e}^{\mathrm{i}k_0 r}/(\epsilon^{\frac{2}{3}}r)$ and hence the leading order terms of the total field near the point Y on Λ_2, u_{FY} say, is obtained, by comparison with equation (3.10) as

$$u_{FY} \sim -\frac{\mathrm{e}^{\mathrm{i}k_0 r}}{\epsilon^{\frac{2}{3}}r}\left\{C_y(y)\rho_2^{\frac{2}{3}}\sin\frac{2\alpha_2}{3} + D_y(y)\rho_2^{\frac{4}{3}}\sin\frac{4\alpha_2}{3}\right\} \quad \text{near } \Lambda_2. \qquad (3.18)$$

At the point under discussion, $y = Y$, $\rho_2 = \epsilon$ and $\alpha_2 = 3\pi/4$, hence

$$G_{FY} \sim -\frac{\mathrm{e}^{\mathrm{i}k_0 r}C_y(Y)}{r}. \qquad (3.19)$$

Applying the reciprocity principle, that the same result is obtained if the source and observer positions are interchanged, shows that

$$G_{YF} = G_{FY} \qquad (3.20)$$

and hence an expression for the unknown function $C_y(Y)$ is obtained as

$$C_y(Y) = -\frac{2\pi}{k_0}f_{1y}(\omega_0; Y), \qquad (3.21)$$

$C_z(Z)$ follows by replacing y, Y with z, Z in (3.21). In order to obtain an expression for $D_y(Y)$, consider first the dipole source of strength $4\pi/\epsilon^{\frac{4}{3}}$, used in the definition of $\hat{G}_{2y}$ (and hence in the limiting case as $\epsilon \to 0$ of G_{2y}) at distance Y along edge Λ_2. The leading order term of the far-field due to *this* source near Λ_2, D_{YF} say, is obtained from the directivity of the dipole edge Green's function, as

$$D_{YF} \sim 2\pi\frac{\mathrm{e}^{\mathrm{i}k_0 r}}{k_0 r}f_{2y}(\omega_0; Y). \qquad (3.22)$$

A second expression for this term is obtained by noting that the source term in the definition of $\hat{G}_{2y}$ is $\epsilon^{-\frac{2}{3}}\partial/\partial\alpha_2$ of the source term in the definition of $\hat{G}_{1y}$. Formally, this is $-\epsilon^{-\frac{2}{3}}\partial/\partial\theta_0$ of the $\hat{G}_{1y}$ source term, where θ_0 is the angular coordinate of the source location. From the reciprocity discussed above, the far-field due to the $\hat{G}_{1y}$ source at θ_0 is the same as the field at θ_0 near to Λ_2 due to the source in the far-field. Hence, the far-field of the dipole source is expressed as

$$\begin{aligned}
D_{YF} &\sim -\frac{1}{\epsilon^{\frac{2}{3}}}\frac{\partial}{\partial\theta_0}\left[-\frac{\mathrm{e}^{\mathrm{i}k_0 r}}{\epsilon^{\frac{2}{3}}r}\left\{C_y(y)\rho_2^{\frac{2}{3}}\sin\frac{2\theta_0}{3} + D_y(y)\rho_2^{\frac{4}{3}}\sin\frac{4\theta_0}{3}\right\}\right]\Bigg|_{\theta_0=\frac{3\pi}{4},y=Y,\rho_2=\epsilon} \\
&= \frac{1}{\epsilon^{\frac{4}{3}}}\frac{\mathrm{e}^{\mathrm{i}k_0 r}}{r}\left\{\frac{2}{3}C_y(y)\rho_2^{\frac{2}{3}}\cos\frac{2\theta_0}{3} + \frac{4}{3}D_y(y)\rho_2^{\frac{4}{3}}\cos\frac{4\theta_0}{3}\right\}\Bigg|_{\theta_0=\frac{3\pi}{4},y=Y,\rho_2=\epsilon}.
\end{aligned}$$
$$(3.23)$$

Hence,

$$D_{YF} = -\frac{4}{3}\frac{\mathrm{e}^{\mathrm{i}k_0 r}}{r}D_y(Y). \tag{3.24}$$

Thus, by equating equations (3.22) and (3.24) the unknown function $D_y(Y)$ is obtained in terms of the dipole directivity as

$$D_y(Y) = -\frac{3}{2}\frac{\pi}{k_0}f_{2y}(\omega_0; Y), \tag{3.25}$$

and $D_z(Z)$ follows by replacing y, Y with z, Z in (3.25). An embedding formula is then obtained for this problem by taking the far-field approximation of the weak embedding formula (3.16), substituting for $C_y(Y)$, $C_z(Z)$, $D_y(Y)$ and $D_z(Z)$, using equations (3.21), (3.25), and noting that $\partial^2/\partial x^2$ corresponds to $-k_0^2\xi^2$ in the far-field, as

$$f(\omega; \omega_0) = \frac{-\pi}{6k_0^3(\xi^2 - \xi_0^2)}\left(\int_0^\infty \{f_{2z}(\omega_0; Z)f_{1z}(\omega; Z) - f_{1z}(\omega_0; Z)f_{2z}(\omega; Z)\}\,\mathrm{d}Z\right.$$
$$\left. + \int_0^\infty \{f_{2y}(\omega_0; Y)f_{1y}(\omega; Y) - f_{1y}(\omega_0; Y)f_{2y}(\omega; Y)\}\,\mathrm{d}Y\right). \tag{3.26}$$

This embedding formula corresponds to Shanin's [12] equation (12) generalised from a flat cone with perpendicular edges to the case of a solid cone with perpendicular faces.

It is useful for practical purposes, that is, for computations such as those in section 2.2, to be able to write this embedding formula in terms of the edge Green's functions on a sphere so they are in a similar form to (2.63). We briefly derive this form of the formulae, to do so we require the spherical coordinates, $\zeta^{x,y,z}, \phi^{x,y,z}$, shown in figure 4, and then we introduce edge Green's functions on a sphere $v_{1z}(\omega, \nu)$ and $v_{2z}(\omega, \nu)$ as the results of limiting procedures:

$$v_{1z}(\omega, \nu) = \lim_{\kappa \to 0}\hat{v}_{1z}(\omega, \nu, \kappa), \qquad v_{2z}(\omega, \nu) = \lim_{\kappa \to 0}\hat{v}_{2z}(\omega, \nu, \kappa), \tag{3.27}$$

where $\hat{v}_{1z}(\omega, \nu, \kappa)$ and $\hat{v}_{2z}(\omega, \nu, \kappa)$ are solutions of the following problems:

$$\tilde{\Delta}_\nu\hat{v}_{1z}(\omega, \nu, \kappa) = \kappa^{-\frac{2}{3}}\frac{1}{\sin\zeta^z}\delta(\zeta^z - \zeta_\kappa)\delta(\phi^z - \phi_\kappa)\text{ on }S, \tag{3.28}$$

$$\hat{v}_{1z}(\omega, \nu, \kappa) = 0\text{ on }\partial S, \tag{3.29}$$

$$\tilde{\Delta}_\nu\hat{v}_{2z}(\omega, \nu, \kappa) = \kappa^{-\frac{4}{3}}\frac{1}{\sin\zeta^z}\delta(\zeta^z - \zeta_\kappa)\delta'(\phi^z - \phi_\kappa)\text{ on }S, \tag{3.30}$$

$$\hat{v}_{2z}(\omega, \nu, \kappa) = 0\text{ on }\partial S \tag{3.31}$$

where S is the surface of the unit sphere without the piece excised by cone, and ∂S is the boundary of S, i.e. the cuts corresponding to cross-sections of
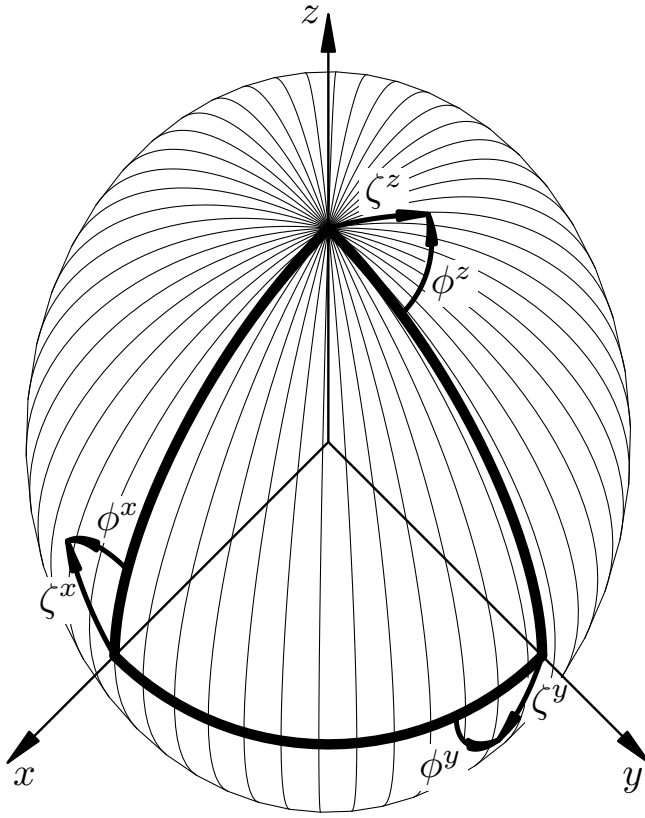
20

Fig. 4. Spherical coordinates for the edge Green's functions.

the cone. The differential operator $\tilde{\Delta}_\nu$ is $\tilde{\Delta}_\nu = \left(\tilde{\Delta} + \nu^2 - \frac{1}{4}\right)$ and $\tilde{\Delta}$ is the angular part of the Laplacian operator, $\zeta_\kappa = \kappa$ and $\phi_\kappa = \frac{3\pi}{4}$. The edge Green's functions $\hat{v}_{1z}(\omega, \nu, \kappa)$ and $\hat{v}_{2z}(\omega, \nu, \kappa)$ are the fields of monopole and dipole point sources placed near the projection of the z-edge of the cone.

Equation (3.26) consists of four terms that are obtained from each other by interchanging variables as $\omega \leftrightarrow \omega_0$ and $z \leftrightarrow y$, so we need only consider the first term

$$\tilde{f}(\omega; \omega_0) = -\frac{\pi}{6k_0^3(\xi^2 - \xi_0^2)} \int_0^\infty f_{2z}(\omega_0, Z) f_{1z}(\omega, Z) dZ. \qquad (3.32)$$

After considerable algebra, and using the properties of the edge Green's functions, in both physical space and in their form on a sphere, one can eventually deduce the first term of the embedding formula in the modified Smyshlyaev form

$$\tilde{f}(\omega; \omega_0) = \frac{i}{12} \frac{1}{(\xi^2 - \xi_0^2)} \int_\Gamma e^{-i\pi\nu} \left(\frac{v_{1z}(\omega, \nu) v_{2z}(\omega_0, \nu - 2) + v_{1z}(\omega, \nu - 2) v_{2z}(\omega_0, \nu)}{\nu - 1} \right.$$

$$\left. -\frac{2\nu}{\nu^2 - 1} v_{1z}(\omega, \nu) v_{2z}(\omega_0, \nu) \right) d\nu \qquad (3.33)$$
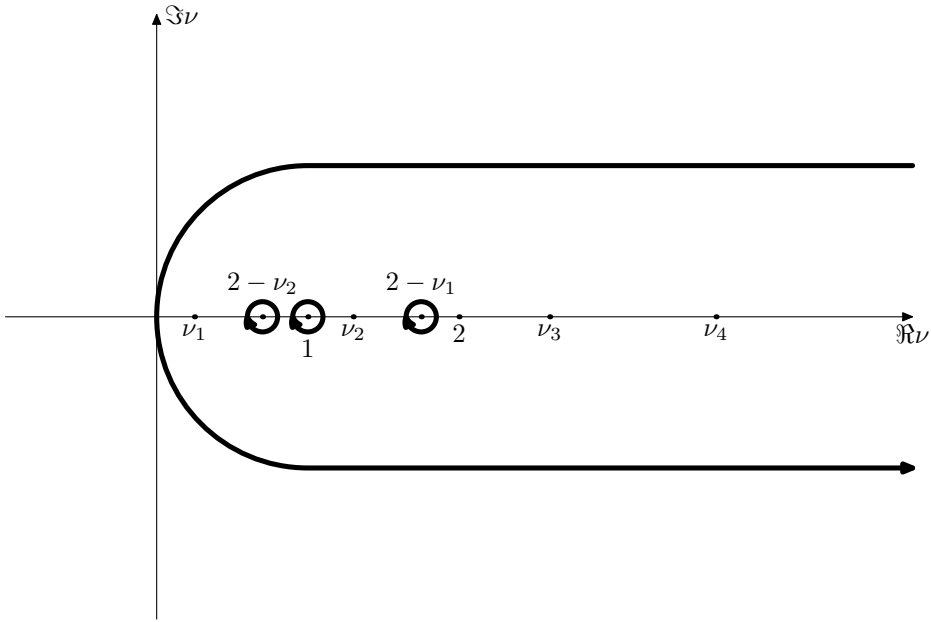
21

Fig. 5. The contour of integration required for the integral in (3.33).

where the contour Γ is shown in figure 5, and thus one can build an expression for $f(\omega; \omega_0)$. Notably the contour is the usual large loop enclosing the positive real axis for ν, but with some poles excluded. The points ν_j and $\nu_j + 2$, where ν_j are the points of the spectrum of the Laplace-Beltrami Dirichlet problem, are all possible poles of the integrand. Potential problems are produced by points 1 and $2 - \nu_j$ for $\nu_j < 2$, and so these points are explicitly excluded from the contour; this is analogous to the subtraction of poles in [12].

3.1.3 Other second order operators

Further embedding formulae are obtained using operators corresponding to differentiation in the other coordinate directions. Thus, making use of the operator

$$H_{2y} = \frac{\partial^2}{\partial y^2} + k_y^2 \tag{3.34}$$

the embedding formula

$$f(\omega; \omega_0) = \frac{-\pi}{6k_0^3(\eta^2 - \eta_0^2)} \left(\int_0^\infty \{f_{2x}(\omega_0; X)f_{1x}(\omega; X) - f_{1x}(\omega_0; X)f_{2x}(\omega; X)\} \, dX \right.$$
$$\left. + \int_0^\infty \{f_{2z}(\omega_0; Z)f_{1z}(\omega; Z) - f_{1z}(\omega_0; Z)f_{2z}(\omega; Z)\} \, dZ \right) \tag{3.35}$$
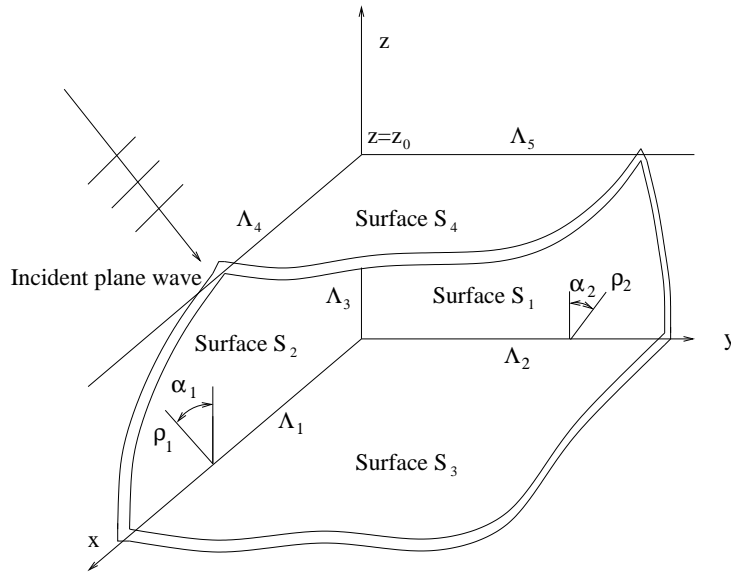
22

Fig. 6. Additional parallel face geometry.

is obtained, and using the operator

$$H_{2z} = \frac{\partial^2}{\partial z^2} + k_0^2(1 - \xi_0^2 - \eta_0^2)$$ (3.36)

the embedding formula

$$f(\omega; \omega_0) = \frac{\pi}{6k_0^3(\xi^2 + \eta^2 - \xi_0^2 - \eta_0^2)} \left(\int_0^\infty \{f_{2x}(\omega_0; X)f_{1x}(\omega; X) - f_{1x}(\omega_0; X)f_{2x}(\omega; X)\} \, dX \right.$$
$$\left. + \int_0^\infty \{f_{2y}(\omega_0; Y)f_{1y}(\omega; Y) - f_{1y}(\omega_0; Y)f_{2y}(\omega; Y)\} \, dY \right)$$ (3.37)

is obtained.

4 Extensions and closing remarks

It becomes clear that the entire embedding procedure can be applied to scattering by quite general shapes. The key being the existence of an operator that kills the incoming field and preserves the boundary conditions. The results of the previous section can be used with only minor alterations for some related geometries. In particular the modification is straightforward if an additional face is present, parallel to one of the existing faces, as shown in figure 6. Suppose that an additional face S_4 is present, parallel to S_3 with $x > 0$, $y > 0$, $z = z_0$, producing edges Λ_4, $x > 0$, $y = 0$, $z = z_0$, and Λ_5, $x = 0$, $y > 0$, $z = z_0$, and the scattering cone occupying $x > 0$, $y > 0$, $0 < z < z_0$. Because

23

the extra faces and edges introduced here are parallel to existing faces and edges the same operators can be used, as they will still preserve the Dirichlet boundary condition on all the faces, and have similar effects on the edges. Any integrations then take place along the length of all relevant edges. Hence, with slightly modified notation for the edge Green's functions and using the operator H_{2x}, the embedding formula

$$
\begin{aligned}
f(\omega;\omega_0) = \frac{-\pi}{6k_0^3(\xi^2 - \xi_0^2)} \bigg(&\int_0^\infty \{f_{2y}(\omega_0; Y, z_0)f_{1y}(\omega; Y, z_0) - f_{1y}(\omega_0; Y, z_0)f_{2y}(\omega; Y, z_0)\}\, \mathrm{d}Y \\
&+ \int_0^\infty \{f_{2y}(\omega_0; Y, 0)f_{1y}(\omega; Y, 0) - f_{1y}(\omega_0; Y, 0)f_{2y}(\omega; Y, 0)\}\, \mathrm{d}Y \\
&+ \int_0^{z_0} \{f_{2z}(\omega_0; Z)f_{1z}(\omega; Z) - f_{1z}(\omega_0; Z)f_{2z}(\omega; Z)\}\, \mathrm{d}Z \bigg)
\end{aligned}
$$

$$(4.1)$$

readily emerges and similar formulae are found if one applies the operator H_{2y} or H_{2z}.

Finally, we can insert more parallel sides (at $x = x_0$ and $y = y_0$) to create a cuboid occupying $0 < x < x_0$, $0 < y < y_0$, $z < z_0$. This results in six faces on which the second order differential operators previously defined still preserve the Dirichlet boundary conditions. There are 12 edges, and for each operator extra terms, as described previously, are required to be included for each operator in order to preserve the edge conditions. The subsequent integrations then take place only along the lengths of the relevant edges. The subsequent result is quite lengthy to reproduce, so only that based on the operator H_{2x} is reproduced here. The results for the operators H_{2y} and H_{2z} are obtained in a completely analogous manner and are omitted here. The embedding formula obtained from the H_{2x} operator is
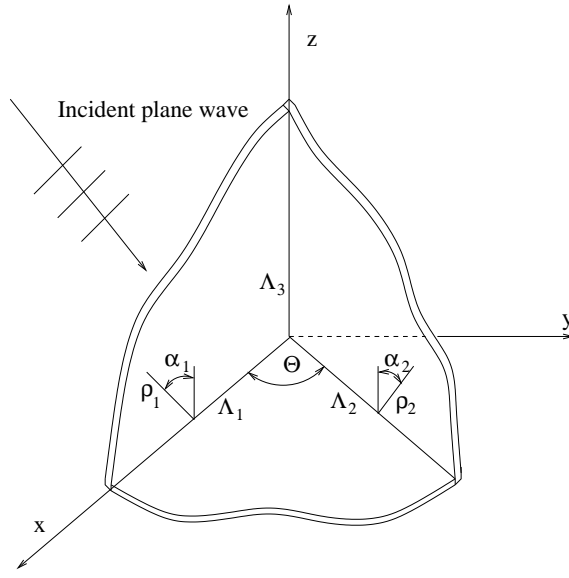
Fig. 7. Cone formed by 2 quarter planes perpendicular to a sector of angle Θ.

$$f(\omega;\omega_0) = \frac{-\pi}{6k_0^3(\xi^2 - \xi_0^2)} \times$$
$$\left(\int_0^{y_0} \{f_{2y}(\omega_0;0,Y,z_0)f_{1y}(\omega;0,Y,z_0) - f_{1y}(\omega_0;0,Y,z_0)f_{2y}(\omega;0,Y,z_0)\} \, \mathrm{d}Y \right.$$
$$+ \int_0^{y_0} \{f_{2y}(\omega_0;x_0,Y,z_0)f_{1y}(\omega;x_0,Y,z_0) - f_{1y}(\omega_0;x_0,Y,z_0)f_{2y}(\omega;x_0,Y,z_0)\} \, \mathrm{d}Y$$
$$+ \int_0^{y_0} \{f_{2y}(\omega_0;0,Y,0)f_{1y}(\omega;0,Y,0) - f_{1y}(\omega_0;0,Y,0)f_{2y}(\omega;0,Y,0)\} \, \mathrm{d}Y$$
$$+ \int_0^{y_0} \{f_{2y}(\omega_0;x_0,Y,0)f_{1y}(\omega;x_0,Y,0) - f_{1y}(\omega_0;x_0,Y,0)f_{2y}(\omega;x_0,Y,0)\} \, \mathrm{d}Y$$
$$+ \int_0^{z_0} \{f_{2z}(\omega_0;0,y_0,Z)f_{1z}(\omega;0,y_0,Z) - f_{1z}(\omega_0;0,y_0,Z)f_{2z}(\omega;0,y_0,Z)\} \, \mathrm{d}Z$$
$$+ \int_0^{z_0} \{f_{2z}(\omega_0;0,0,Z)f_{1z}(\omega;0,0,Z) - f_{1z}(\omega_0;0,0,Z)f_{2z}(\omega;0,0,Z)\} \, \mathrm{d}Z$$
$$+ \int_0^{z_0} \{f_{2z}(\omega_0;x_0,0,Z)f_{1z}(\omega;x_0,0,Z) - f_{1z}(\omega_0;x_0,0,Z)f_{2z}(\omega;x_0,0,Z)\} \, \mathrm{d}Z$$
$$\left. + \int_0^{z_0} \{f_{2z}(\omega_0;x_0,y_0,Z)f_{1z}(\omega;x_0,y_0,Z) - f_{1z}(\omega_0;x_0,y_0,Z)f_{2z}(\omega;x_0,y_0,Z)\} \, \mathrm{d}Z \right).$$

(4.2)

Thus, the integrations take place along the edges where the variable is y or z.

We now relax the requirement that all edges are mutually perpendicular and move the edge Λ_2 in the x–y plane away from the y-axis to make angle Θ with the x-axis, as shown in figure 7. Thus the surface S_3 is the same surface as in the flat cone example of a previous section. It is now necessary to find a suitable differential operator preserving the Dirichlet boundary condition on the faces S_1, S_2 and S_3, and then to determine a suitable combination of monopoles, dipoles ... to assemble along the edges to satisfy the edge conditions.

25

It is simplest to choose an operator based on $\partial/\partial z$ and to proceed as before. This preserves the Dirichlet boundary condition on surfaces S_1 and S_2, and since the angle between each of these surfaces and S_3 is still $\pi/2$, the operator H_{2z} based on $T_2(\partial/\partial z)$ preserves the Dirichlet boundary condition on all three surfaces. On the edge Λ_3 the operator H_{2z} preserves the edge condition. On the edge Λ_1 the behaviour is that described previously for the octant case. Similarly, since the angle between faces S_1 and S_3 is also $\pi/2$ it can be deduced that the behaviour near the edge Λ_2 has similar characteristics to that near Λ_1. Thus, the embedding formula is obtained in this case as

$$
f(\omega;\omega_0) = \frac{\pi}{6k_0^3(\xi^2 + \eta^2 - \xi_0^2 - \eta_0^2)} \left(\int_0^\infty \{f_{2x}(\omega_0;X)f_{1x}(\omega;X) - f_{1x}(\omega_0;X)f_{2x}(\omega;X)\}\,\mathrm{d}X \right.
$$
$$
\left. + \int_0^\infty \{f_{2s}(\omega_0;S)f_{1s}(\omega;S) - f_{1s}(\omega_0;S)f_{2s}(\omega;S)\}\,\mathrm{d}S \right).
$$
(4.3)

This is of the same form as (3.37), but with the variable Y for the integration replaced by S, the variable measured along Λ_2, and the Green's functions f_{1x}, f_{2x}, f_{1s} and f_{2s} are those for *this* cone shape.

Hence, we see that a combination of the ideas used in this article can be utilised to consider scattering by quite general geometries. Moreover, it is not unusual for there to be several embedding formulae and these can be used to cross-validate the results. However, we sound a note of warning, unlike the octant or cuboid discussed previously, for the cone in figure 7 other embedding formulae cannot be obtained merely by interchanging the coordinate for the differentiation in the operator, i.e. H_{2x} and H_{2y} or H_{2s} are not in general suitable for obtaining an embedding formula. To see this consider the operator H_{2x}, it does not in general preserve the Dirichlet boundary condition on the face S_1. However, as Λ_1 and Λ_2 are both perpendicular to Λ_3, the face S_2 can be rotated around Λ_3 onto the face S_1. An operator based on this angle may preserve the Dirichlet boundary condition on S_1. However, for example, if $\Theta = \pi/3$ then even the operator H_{3x} does not in general preserve the Dirichlet boundary condition on S_1 and is not a suitable operator. In addition to preserving the Dirichlet boundary conditions on the faces a suitable operator for obtaining an embedding formula is also required to produce edge behaviour which can be expressed in terms of edge Green's functions (monopoles and higher orders). In this example the direction of the differentiation is neither parallel to nor perpendicular to the edge Λ_2 and is also not in the plane of one of the faces there, hence considerably more analysis is needed to investigate the edge behaviour there and to determine suitable operators for this geometry.

In conclusion it is therefore clear that scattering from many three-dimensional geometries can be considered using the embedding formulae philosophy es-

poused in [22] and subsequent articles. The embedding is far easier for planar structures, but can be generalised to right-angled geometries reasonably straightforwardly. Even more general angled structures can be contemplated, but the identification of the appropriate operator becomes more arduous. None the less the fact that embedding can be utilised suggests that this route could dramatically reduce the effort required to generate far-field directivity functions for these geometries.

5 Acknowledgements

References

[1] J. B. Keller, The geometric theory of diffraction, J. Opt. Soc. Amer. 52 (1962) 116–130.

[2] A. V. Osipov, A. N. Norris, The Malyuzhinets theory for scattering from wedge boundaries: a review, Wave Motion 29 (1999) 313–340.

[3] B. Noble, Methods based on the Wiener-Hopf technique, Pergamon Press, 1958.

[4] D. S. Jones, Acoustic and electromagnetic waves, Oxford University Press, 1986.

[5] L. B. Felsen, N. Marcuvitz, Radiation and scattering of waves, Prentice-Hall, 1973.

[6] L. Kraus, L. M. Levine, Diffraction by an elliptic cone, Comm. Pure Appl. Math. 14 (1961) 49–68.

[7] S. Blume, U. Uschkerat, The radar cross-section of the semi infinite elliptic cone - numerical evaluation, Wave Motion 22 (1995) 311–326.

[8] V. P. Smyshlyaev, Diffraction by conical surfaces at high frequencies, Wave Motion 12 (1990) 329–339.

[9] V. P. Smyshlyaev, The high-frequency diffraction of electromagnetic waves by cones of arbitrary cross sections, SIAM J. Appl. Math. 53 (1993) 670–688.

[10] V. M. Babich, D. B. Dementév, B. A. Samokish, V. P. Smyshlyaev, On evaluation of the diffraction coefficients for arbitrary nonsingular directions of a smooth convex cone, SIAM J. Appl. Math. 60 (2000) 536–573.

[11] B. D. Bonner, I. G. Graham, V. P. Smyshlyaev, The computation of conical diffraction coefficients in high-frequency acoustic wave scattering, SIAM J. Num. Anal. 43 (2005) 1202–1230.

[12] A. V. Shanin, Modified Smyshlyaev's formulae for the problem of diffraction of a plane wave by an ideal quarter plane, Wave Motion 41 (2005) 79–93.

[13] R. V. Craster, A. N. Shanin, Embedding formulae for diffraction by rational wedge and angular geometries, Proc. R. Soc. Lond. A 461 (2005) 2227–2242.

[14] M. H. Williams, Diffraction by a finite strip, Q. Jl. Mech. Appl. Math. 35 (1982) 103–124.

[15] A. K. Gautesen, On the Green's function for acoustical diffraction by a strip, J. Acoust. Soc. Am. 74 (1983) 600–604.

[16] P. A. Martin, G. R. Wickham, Diffraction of elastic waves by a penny-shaped crack: analytical and numerical results, Proc. R. Soc. Lond. A 390 (1983) 91–129.

[17] C. M. Linton, P. McIver, Handbook of mathematical techniques for wave/structure interactions, Chapman-Hall CRC Press, 2001.

[18] N. R. T. Biggs, D. Porter, D. S. G. Stirling, Wave diffraction through a perforated breakwater, Q. Jl. Mech. appl. Math. 53 (2000) 375–391.

[19] N. R. T. Biggs, D. Porter, Wave diffraction through a perforated barrier of non-zero thickness, Q. Jl. Mech. appl. Math. 54 (2001) 523–547.

[20] N. R. T. Biggs, D. Porter, Wave scattering by a perforated duct, Q. Jl. Mech. Appl. Math. 55 (2002) 249–272.

[21] N. R. T. Biggs, D. Porter, Wave scattering by an array of perforated breakwaters, IMA J. Appl. Math. 70 (2005) 908–936.

[22] R. V. Craster, A. V. Shanin, E. M. Doubravsky, Embedding formulae in diffraction theory, Proc. R. Soc. Lond. A 459 (2003) 2475–2496.

[23] E. A. Skelton, R. V. Craster, A. V. Shanin, Embedding formulae for diffraction by non-parallel slits, Q. Jl. Mech. Appl. Math. 61 (2008) 93–116.

[24] N. R. T. Biggs, A new family of embedding formulae for diffraction by wedges and polygons, Wave Motion 43 (2006) 517–528.

[25] A. V. Shanin, Coordinate equations for a problem on a sphere with a cut associated with diffraction by an ideal quarter plane, Q. J. Mech. Appl. Math. 58 (2005) 289–308.

A   Appendix: Local behaviour of a monopole point or dipole source near the edge of a wedge of rational angle

In the text we require edge Green's functions and their behaviour in the near field, to obtain this it is necessary to consider some source and wedge interaction problems and the purpose of this appendix is to sketch the derivation of the near field.

We treat the monopole source is detail. The Helmholtz wave equation is satisfied by fluid outside an infinitely long wedge whose angle is a rational multiple of π, $p\pi/q$, as shown in figure A.1. Cylindrical polar coordinates (r, θ, z), where the z-axis coincides with the vertex edge, r is measured from the vertex, and θ is measured from one of the wedge faces are used. A point source is located in the fluid midway between the wedge faces, at radial distance r_0 from the vertex line. Thus, the governing equations for u are

$$(\nabla^2 + k_0^2)u_1(\mathbf{R}; \mathbf{R_0}) = -4\pi\delta(r-r_0)\delta(\theta-\theta_0)\delta(z-z_0)/r_0, \quad 0 < \theta < 2\theta_0, \quad \text{(A.1)}$$

in which

$$\theta_0 = \pi(1 - p/2q), \tag{A.2}$$

together with the Dirichlet boundary conditions on the wedge faces

$$u_1(\mathbf{R}; \mathbf{R_0}) = 0 \quad \text{at} \quad \theta = 0 \quad \text{and} \quad \theta = 2\theta_0. \tag{A.3}$$

Utilising a Fourier series expansion in θ, a Hankel transform in radius, r, and a Fourier transform in the axial direction z the following solution, for $r \geq r_0 > 0$, emerges

$$u_1(\mathbf{R}; \mathbf{R_0}) = \frac{-\pi i}{\theta_0} \sum_{\substack{n=1 \\ n \text{ odd}}}^{\infty} \sin\left(\frac{n\pi\theta}{2\theta_0}\right) \sin\left(\frac{n\pi}{2}\right) \int_{-\infty}^{\infty} J_{\frac{n\pi}{2\theta_0}}(\gamma r_0) H_{\frac{n\pi}{2\theta_0}}(\gamma r) e^{i\alpha(z-z_0)} d\alpha,$$

$$\text{(A.4)}$$

in which $\gamma = \sqrt{k_0^2 - \alpha^2}$. As the source approaches the edge of the wedge $r_0 \to 0$ and the leading order term of $u_1(\mathbf{R}; \mathbf{R_0})$ results from the $n = 1$ term of the
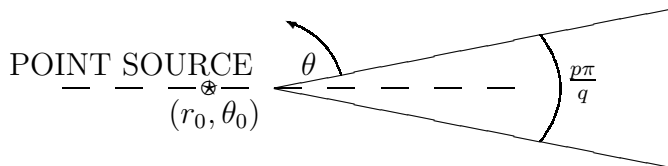

Fig. A.1. Wedge geometry

29

summation:

$$u_1(\mathbf{R};\mathbf{R_0}) \sim \frac{-\pi\mathrm{i}}{\theta_0\Gamma\left(\frac{\pi}{2\theta_0}+1\right)} \left(\frac{r_0}{2}\right)^{\frac{\pi}{2\theta_0}} \sin\left(\frac{\pi\theta}{2\theta_0}\right) \int_{-\infty}^{\infty} \gamma^{\frac{\pi}{2\theta_0}} \mathrm{H}_{\frac{\pi}{2\theta_0}}(\gamma r)\mathrm{e}^{\mathrm{i}\alpha(z-z_0)}\mathrm{d}\alpha.$$

(A.5)

It is frequently useful to consider a source whose strength varies as $r_0^{-\pi/2\theta_0}$ and then to use the limit as $r_0 \to 0$. This limiting case is obtained by omitting the $r_0^{\pi/2\theta_0}$ factor above and replacing the '$\sim$' with '$=$':

$$u_{1\mathrm{lim}}(\mathbf{R};z_0) = \frac{-\pi\mathrm{i}}{\theta_0\Gamma\left(\frac{n\pi}{2\theta_0}+1\right)} \left(\frac{1}{2}\right)^{\frac{\pi}{2\theta_0}} \sin\left(\frac{\pi\theta}{2\theta_0}\right) \int_{-\infty}^{\infty} \gamma^{\frac{\pi}{2\theta_0}} \mathrm{H}_{\frac{\pi}{2\theta_0}}(\gamma r)\mathrm{e}^{\mathrm{i}\alpha(z-z_0)}\mathrm{d}\alpha.$$

(A.6)

In this exposition the $r_0^{\pi/2\theta_0}$ factor will be retained, but with the understanding that the limit procedure will be subsequently applied. Next, the near field behaviour of equation (A.6) as $r \to 0$ is examined, using known properties of Hankel functions, and

$$u_1(\mathbf{R};\mathbf{R_0}) \sim \frac{-\Gamma\left(\frac{\pi}{2\theta_0}\right)}{\theta_0\Gamma\left(\frac{\pi}{2\theta_0}+1\right)} \left(\frac{r_0}{r}\right)^{\frac{\pi}{2\theta_0}} \sin\left(\frac{\pi\theta}{2\theta_0}\right) \int_{-\infty}^{\infty} \left\{1 + A\gamma^2 r^2 + \ldots\right\} \mathrm{e}^{\mathrm{i}\alpha(z-z_0)}\mathrm{d}\alpha.$$

(A.7)

as $r \to 0$. Inverting the Fourier transforms using delta functions and their derivatives yields the near field behaviour of $u_1(\mathbf{R};\mathbf{R_0})$ as

$$u_1(\mathbf{R};\mathbf{R_0}) \sim -4\left(\frac{r_0}{r}\right)^{\frac{\pi}{2\theta_0}} \sin\left(\frac{\pi\theta}{2\theta_0}\right) \left\{\left(1 + Ak_0^2 r^2 + \ldots\right)\delta(z-z_0)\, ,\right.$$

$$\left. + \left(Ar^2 + \ldots\right)\delta''(z-z_0) + \ldots\right\}.$$

(A.8)

This form of the solution is particularly useful for evaluating integrals with respect to z_0, for example, as $r \to 0$

$$\int_0^{\infty} h(Z)u_1(r,\theta,z;r_0,\theta_0,Z)\mathrm{d}Z \sim 4\left(\frac{r_0}{r}\right)^{\frac{\pi}{2\theta_0}} \sin\left(\frac{\pi\theta}{2\theta_0}\right)$$

$$\left\{\left(1 + Ak_0^2 r^2 + \ldots\right)h(z) + \left(Ar^2 + \ldots\right)h''(z) + \ldots\right\}.$$

(A.9)

For the dipole, the inhomogeneous Helmholtz equation (A.1) is replaced by

$$(\nabla^2 + k_0^2)u_2(\mathbf{R};\mathbf{R_0}) = -4\pi\delta(r-r_0)\delta'(\theta-\theta_0)\delta(z-z_0)/r_0, \quad 0 < \theta < 2\theta_0, \quad \text{(A.10)}$$

and following through the analysis above gives the near field for the dipole as

$$u_2(\mathbf{R};\mathbf{R_0}) \sim \frac{-2\pi}{\theta_0}\left(\frac{r_0}{r}\right)^{\frac{\pi}{\theta_0}} \sin\left(\frac{\pi\theta}{\theta_0}\right)$$

$$\left\{\left(1 + Bk_0^2 r^2 + \ldots\right)\delta(z-z_0) + \left(Br^2 + \ldots\right)\delta''(z-z_0) + \ldots\right\}.$$

(A.11)

30

Hence the near field behaviour of the required integrals with respect to z_0 are obtained as

$$\int_0^\infty h(Z)u_2(r, \theta, z; r_0, \theta_0, Z)\mathrm{d}Z \sim \frac{2\pi}{\theta_0} \left(\frac{r_0}{r}\right)^{\frac{\pi}{\theta_0}} \sin\left(\frac{\pi\theta}{\theta_0}\right)$$

$$\left\{\left(1 + Bk_0^2r^2 + \ldots\right)h(z) + \left(Br^2 + \ldots\right)h''(z) + \ldots\right\}, \quad \text{as } r \to 0. \quad \text{(A.12)}$$